Journal of Molecular Structure 919 (2009) 343–347

Contents lists available at ScienceDirect

Journal of Molecular Structure

journal homepage: www.elsevier.com/locate/molstruc

Sulfur tetrafluoride methylimide, $CH_3N{=}SF_4$: Vibrational spectra and quantum chemical calculations ☆

Ana G. Iriarte [a], Edgardo H. Cutin [a], Rosa M.S. Álvarez [a,*], Rüdiger Mews [b], Heinz Oberhammer [c,*]

[a] Instituto de Química Física, Facultad de Bioquímica, Química y Farmacia, Universidad Nacional de Tucumán, San Lorenzo 456, (4000) Tucumán, Argentina
[b] Institut für Anorganische und Physikalische Chemie, Universität Bremen, 28334 Bremen, Germany
[c] Institut für Physikalische und Theoretische Chemie, Universität Tübingen, 72076 Tübingen, Germany

ARTICLE INFO

Article history:
Received 1 August 2008
Received in revised form 1 October 2008
Accepted 2 October 2008
Available online 12 October 2008

Keywords:
Sulfur tetrafluoride methylimide
Vibrational spectra
Quantum chemical calculations

ABSTRACT

Infrared (gas) and Raman (liquid) spectra of sulfur tetrafluoride methylimide, $CH_3N{=}SF_4$, were recorded and interpreted. Structural, vibrational and configurational properties were derived from quantum chemical calculations [HF, MP2 and B3LYP methods with 6-311+G(2df,p) basis sets]. The assignment of the normal modes of vibrations was carried out by comparison with analogous molecules and with calculated frequencies and intensities. All theoretical approaches predict the existence of a unique form in the fluid phases which possesses C_S symmetry, in good agreement with experimental results.

1. Introduction

During the past years our group has been interested in the study of structural and vibrational properties of sulfur-nitrogen compounds, particularly those containing tri-coordinate and tetra-coordinate sulfur atoms. Thus, series of imido compounds of the type $RN{=}SX_2$ (X=Cl, F, CF_3; R=FCO, CF_3, CF_3CO, FSO_2, $ClSO_2$, CN) [1–6] and oxide difluoride imides of the type $RN{=}SOF_2$ (R=FCO, CN, SFO_2, F_5S) [7–10] have been analysed by infrared and Raman spectroscopy, by joint analyses of gas electron diffraction (GED) and microwave spectroscopy and by quantum chemical calculations at different levels of theory. In order to extent this series of sulfur–nitrogen molecules, we now start the study of systems containing penta-coordinated S(VI). We are interested particularly in studying sulfur tetrafluoride imides, since only few members of this class of compounds are known.

In this context, we present here a vibrational analysis of sulfur tetrafluoride methylimide, $CH_3N{=}SF_4$, based on the observed features in the IR and Raman spectra of the compound and supported by quantum chemical predictions of its vibrational behaviour. This study completes the structural analysis for this compound, based on gas electron diffraction, microwave and NMR spectroscopy, which was published by Günther et al. [11]. Results derived from this structural analysis were consistent with the presence of a unique stable structure with the CH_3 group in axial orientation, i.e. in the axial plane of the SF_4 group, and with the N=S bond in the equatorial plane of the SF_4 group (see Chart 1). It was also reported, that the mean axial bond length is larger than the equatorial one, as was observed in related molecules, like $O{=}SF_4$ [12] and $CH_2{=}SF_4$ [13]. Furthermore, the axial S—F bond in *syn* orientation with respect to the nitrogen lone pair is considerably shorter than the axial bond in the direction of the nitrogen substituent. These different axial S—F bond lengths were rationalized by distortion of the bipyramidal SF_4 entity from C_{2v} to C_S symmetry, due to the presence of the nitrogen substituent.

2. Experimental

$CH_3N{=}SF_4$ was prepared according to the method reported in reference [14]. The gas FTIR spectrum was registered with a Bruker IFS 66v FTIR spectrometer by using a 10 cm path-length cell equipped with KBr windows (pressure: 2 Torr, resolution 1 cm^{-1}). A Bruker RFS 100/S FT Raman spectrometer was used to obtain the liquid Raman spectrum of the $CH_3N{=}SF_4$ molecule (resolution 2 cm^{-1}). The liquid sample was handled in glass capillaries at room temperature.

3. Quantum chemical calculations

The geometric structure of $CH_3N{=}SF_4$ was optimized with HF, MP2 and B3LYP methods and 6-311+G(2df,p) basis sets. The

☆ EHC and RMSA are members of the Carrera del Investigador Científico y Tecnológico del Consejo Nacional de Investigaciones Científicas y Técnicas (CONICET), República Argentina. AGI is a doctoral fellow of CONICET, República Argentina.

* Corresponding authors. Tel.: +54 381 4213226.
E-mail addresses: mysuko@fbqf.unt.edu.ar (R.M.S. Álvarez), heinzoberhammer@uni-tuebingen.de (H. Oberhammer).

0022-2860/$ - see front matter © 2008 Elsevier B.V. All rights reserved.
doi:10.1016/j.molstruc.2008.10.004

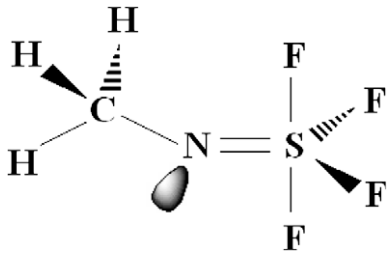

Chart 1.

structure with atom numbering is shown in Fig. 1 and geometric parameters are summarized in Table 1 together with experimental values derived by a combined gas electron diffraction/microwave study. Vibrational frequencies and relative intensities were calculated with the same methods and are included in Table 2.

The calculations result in staggered orientation of the CH_3 group relative to the N=S bond. This is in contrast to the experimental result where an eclipsed orientation was slightly favoured. However, microwave rotational constants do not depend on the orientation of the methyl group and electron diffraction intensities are rather unsensitive towards the orientation of this group. A noteworthy structural feature of $CH_3N{=}SF_4$ is the strong distortion of the SF_4 group from C_{2v} to C_S symmetry. The experimental difference between the N=S—F1 and N=S—F2 angles of 3.8(0.6)° is well reproduced by the calculations (4.0–5.3°). On the other hand, the large experimental difference between the two axial S—F bond lengths, (S—F1)—(S—F2) = 0.097(9) Å, is underestimated by these calculations. Predicted differences vary between 0.037 (HF) and 0.055 Å (B3LYP). Intuitively, the long S—F1 bond which is oriented trans to the nitrogen lone pair and cis to the N—CH_3 bond (see Chart 1 and Fig. 1) could be interpreted by a strong orbital interaction (anomeric effect) between the nitrogen lone pair and the antibonding S—F1 orbital, lp(N)→σ*(S—F1). This interaction is expected to populate the σ*(S—F1) orbital and, thus, to lengthen this bond. However, a natural bond orbital (NBO) analysis which was performed with the MP2 wave function demonstrates that the orbital interaction between the nitrogen lone pair and the *cis* oriented S—F2 bond is stronger than that with the *trans* orientated S—F1 bond. Thus, this anomeric effect would lead to a longer S—F2 bond compared to S—F1, in contrast to experimental and theoretical results. On the other hand, the NBO population of the σ*(S—F1) orbital is indeed higher than that of the σ*(S—F2) orbital, in agreement with the longer S—F1 bond. A detailed analysis of the NBO interactions reveals that the higher population of the σ*(S—F1) orbital is predominantly due to interactions with the σ orbitals of the S=N and of the equatorial S—F bonds.

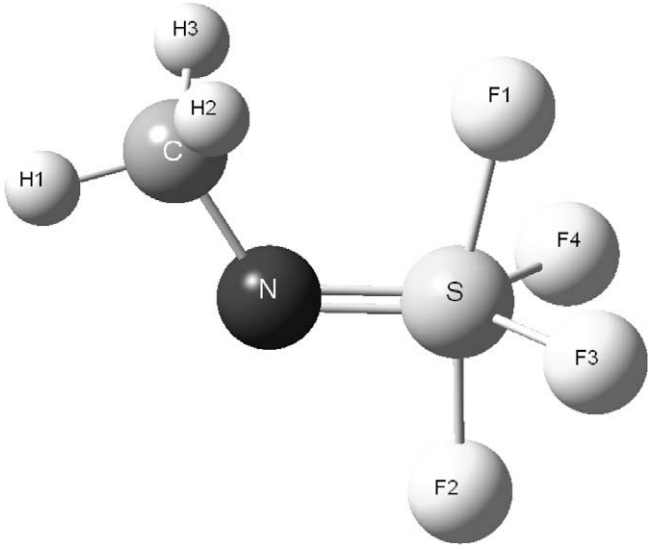

Fig. 1. Molecular model for $CH_3N{=}SF_4$.

Table 1
Principal Experimental and Calculated Geometric Parameters for $CH_3N{=}SF_4$[a] (without parameters defining positions of hydrogen atoms).

	Experimental data[b]	Theoretical data		
		HF/6-311+G(2df,p)	MP2/6-311+G(2df,p)	B3LYP/6-311+G(2df,p)
N=S	1.480(6)	1.460	1.494	1.495
S—F3,4	1.567(4)	1.518	1.567	1.587
S—F1	1.643(4)	1.590	1.640	1.660
S—F2	1.546(7)	1.553	1.591	1.605
N—C	1.441(16)	1.456	1.464	1.466
F3SF4	102.6(0.2)	104.7	103.1	103.0
NSF1	98.4(0.4)	98.5	99.1	99.3
NSF2	94.6(0.4)	94.5	93.8	94.1
F1SF2	167.0(0.6)	166.8	167.0	166.6
SNC	127.2(1.1)	125.1	122.2	123.8

[a] Bond lengths in Å and angles in degrees. See Fig. 1 for atom numbering.
[b] See Ref. [11]

In addition to these calculations, the potential function for pseudorotation was derived with the B3LYP/6-311+G(2df,p) method by optimizing structures for various fixed equatorial F–S–F angles. With increasing equatorial bond angle rotation around the S=N bond by 90° from the initial axial orientation to the final axial orientation occurs. The predicted barrier to pseudorotation is 11.9 kcal/mol, slightly higher than the experimental value of 10.0 kcal/mol, which was estimated from the approximate coalescence temperature of −30 °C in the NMR spectra [11]. All calculations were performed with the GAUSSIAN03 program system [15].

4. Vibrational spectra

Infrared and Raman spectra of the gaseous and liquid phases, respectively, which were recorded at room temperature, are shown in Fig. 2. The observed features in the IR and Raman spectra are consistent with the existence of a single conformer. Thus, a structure possessing C_S symmetry, as derived by theoretical calculations and by previous experiments [11] was used in the analysis of the vibrational spectra. The expected 24 normal modes of vibration have been assigned on the basis of characteristic wavenumbers and taking into account the calculated vibrational frequencies and intensities for this compound. In addition, molecules possessing the CH_3N— and —N=SF_4 moieties were considered as reference of vibrational behaviour. Thus, experimental and calculated frequencies of $CH_3N{=}S(CF_3)_2$ [16] and $CH_3N{=}S(F_2){=}NCH_3$ [17], as well as theoretical vibrational spectra obtained for $FN{=}SF_4$ and $CF_3N{=}SF_4$ were used in the analysis of the fundamental modes. Table 2 lists the experimental and calculated wavenumbers together with a tentative assignment for $CH_3N{=}SF_4$. In general, good agreement exists between the experimental and the calculated frequencies and relative intensities derived by the different methods (HF (scaled by 0.9) and unscaled B3LYP and MP2 values derived with the 6-311+G(2df,p) basis sets). Some experimental wavenumbers were reproduced closer by the B3LYP method, others by the MP2 approximation.

At the highest wavenumbers in the vibrational spectra of $CH_3N{=}SF_4$ three bands were observed, which could straightforwardly be associated with the two asymmetric and the one symmetric stretching modes of the CH_3 group. They are centered at

Table 2
Experimental and calculated wavenumbers (cm^{-1}), and tentative assignments of the fundamental modes for $CH_3N{=}SF_4$.

Mode	Approximate description[a]	Experimental[b]		Calculated[c]		
		IR (gas)	Raman (liquid)	HF 6-311+G (2df,p)[d]	B3LYP 6-311++G (2df,p)	MP26-311+G(2df,p)
ν_1 (A′)	CH_3 asym. stretch.	3007 (28)	3006 (12)	2945 (4)	3126 (2)	3195 (1)
ν_2 (A″)	CH_3 asym. stretch.	2966 (41)	2961 (47)	2929 (5)	3118 (3)	3184 (2)
ν_3 (A′)	CH_3 sym. stretch.	2914 (20)	2904 (14)	2871 (10)	3049 (8)	3090 (6)
ν_4 (A″)	CH_3 rocking	1473 (29)	1475sh (6)	1466 (1)	1499 (2)	1527 (2)
ν_5 (A′)	CH_3 scissoring	1462 (28)	1464 (8)	1455 (5)	1491 (3)	1514 (<1)
ν_6 (A′)	CH_3 sym. def.	1437 (18)	1433 (6)	1436 (<1)	1465 (<1)	1479 (<1)
ν_7 (A′)	N═S stretch.	1313 (98)	1302 (15)	1329 (92)	1300 (64)	1351 (63)
ν_8 (A′)	CH_3 wagging	–	1127 (5)	1132 (<1)	1145 (<1)	1160 (<1)
ν_9 (A″)	CH_3 twisting	–	1127 (5)	1120 (<1)	1136 (<1)	1152 (<1)
ν_{10} (A′)	C—N stretch.	951 (95)	945 (3)	958 (39)	937 (35)	978 (33)
ν_{11} (A″)	FSF eq. asym. stretch.	854 (98)	843 (4)	895 (53)	802 (55)	851 (54)
ν_{12} (A′)	FSF ax. asym. stretch.	816 (100)	781 (6)	828 (100)	785 (100)	823 (100)
ν_{13} (A′)	SF_4 sym. stretch.	716 (74)	710 (100)	757 (7)	677 (19)	715 (16)
ν_{14} (A′)	NSF eq. o.o.pl. def.	621 (36)	617 (8)	623 (8)	596 (3)	616 (4)
ν_{15} (A′)	SF_4 sym. def.	560 (58)	550 (11)	580 (2)	534 (3)	561 (3)
ν_{16} (A′)	SF_4 asym. stretch.	513 (68)	511 (20)	562 (7)	522 (5)	550 (6)
ν_{17} (A′)	NSF_4 wagging	–	493 (17)	532 (<1)	496 (7)	516 (<1)
ν_{18} (A″)	SF eq. Rocking	–	493 (17)	525 (<1)	493 (<1)	511 (6)
ν_{19} (A″)	SF ax. Rocking	–	–	505 (7)	470 (2)	497 (2)
ν_{20} (A′)	NSC i.pl. def.	–	268 (12)	287 (<1)	268 (2)	287 (2)
ν_{21} (A″)	NSC o.o.pl. def.	–	243 (14)	267 (1)	266 (<1)	273 (<1)
ν_{22} (A′)	FSF scissoring	–	151 (14)	245 (<1)	229 (<1)	244 (<1)
ν_{23} (A″)	CH_3NS torsion	–	83 (11)	123 (<1)	138 (<1)	155 (<1)
ν_{24} (A″)	CH_3 torsion	–	56 (8)	58 (<1)	97 (<1)	142 (<1)

[a] stretch, stretching; def., deformation; o.o.pl., out-of-plane; i.pl., in-plane asym., asymmetric; sym.; symmetric, eq., equatorial; ax., axial.
[b] gas: relative absorbance at band maximum in parentheses; liquid: relative band intensity in parentheses. sh: shoulder.
[c] Relative calculated infrared band strength in parentheses.
[d] Scaled by the factor 0.9.

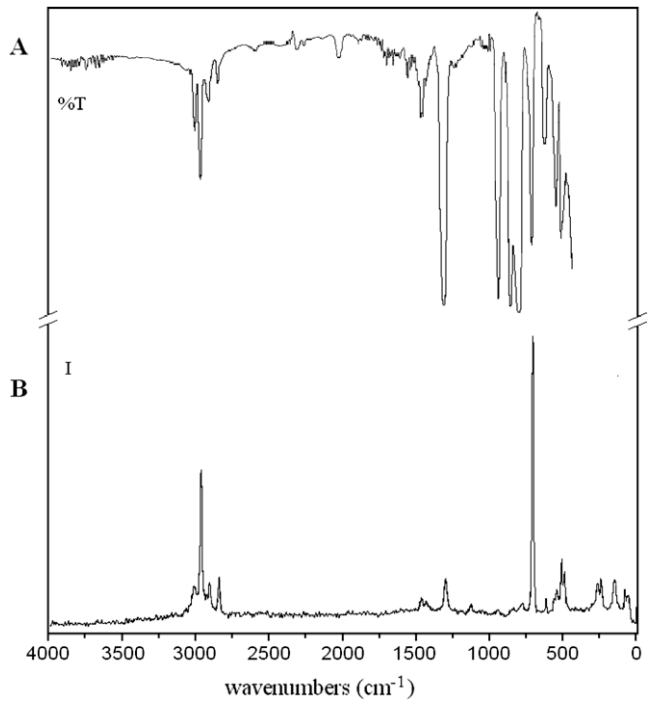

Fig. 2. (A) Gas phase infrared, pressure 2 Torr (resolution 1 cm^{-1}) and (B) liquid Raman spectra of $CH_3N{=}SF_4$ (resolution 2 cm^{-1}).

3007, 2966 and 2914 cm^{-1} in the gas IR spectrum. In $CH_3N{=}S(F_2){=}NCH_3$ these normal vibrations were observed at 3003, 2953 and 2922 cm^{-1}[17], while for $CH_3N{=}S(CF_3)_2$ the bands were centered at slightly lower frequencies, 2994, 2937 and 2890 cm^{-1}, respectively [16], demonstrating good agreement among them. This region shows an additional band located at 2845 (IR) and 2839 cm^{-1} (Ra), which was assigned to the overtone of the symmetric CH_3 deformation mode (ν_6) in Fermi resonance with the symmetric stretching (ν_3). Similar behaviour was observed in the reference molecules containing the CH_3 group, such as $CH_3N{=}S(CF_3)_2$, where the reported frequencies are 2815 and 2811 cm^{-1} (IR and Raman, respectively) [16] and $CH_3N{=}S(F_2){=}NCH_3$, where this overtone was observed at 2862 (IR) and 2844 cm^{-1} (Raman) [17].

The characteristic features belonging to the CH_3 deformation modes are expected in the region between 1480 and 1400 cm^{-1}. The weak signals observed at 1473, 1462 and 1437 cm^{-1} in the IR were associated with the rocking, scissoring and symmetric deformation modes of the CH_3 group, in good agreement with the reported values for $CH_3N{=}S(CF_3)_2$, (1473, 1458 and 1420 cm^{-1}, respectively) [16], and with those observed in $CH_3N{=}S(F_2){=}NCH_3$, (1460, 1433 and 1410 cm^{-1}, respectively) [17]. These three fundamental modes experimentally observed in the IR and Raman spectra are well reproduced by the calculations for title and reference molecules. The two remaining CH_3 deformation modes of $CH_3N{=}SF_4$ were not observed in the IR spectrum, in accordance with the calculations which predict very weak features at 1145 and 1136 cm^{-1}. In the Raman spectrum they appear as a weak signal centered at 1127 cm^{-1}.

A very strong IR band and a medium-intensity Raman signal are associated with the N═S stretching mode. It is interesting to point out that the location of this vibration depends very strongly on the electronegativity of the groups attached to N and to S and also on the sulfur hybridization. We observed this fundamental in a very wide spectral range around 1300 cm^{-1} and a general correlation between the wavenumbers of the N═S stretching mode and the corresponding bond lengths is observed for molecules possessing the $CH_3N{=}S$-moiety [16,17] with S(IV) or S(VI) in tri-coordinated (—SX_2; X═F; CF_3), tetra-coordinated (—SF_2NCH_3) or penta-coordinated (—SF_4) states. Table 3 lists gas IR bands corresponding to the N═S stretching mode and calculated bond lengths (B3LYP/6-311+G(2df,p)) for RN═S—(R═CH_3, CF_3) containing molecules. The

Table 3
Experimental and/or calculated N=S and N–C stretching wavenumbers and calculated N=S bond lengths for some molecules containing the C–N=S entity.

Molecule	ν(N=S)[a] (cm^{-1})	N=S (Å)[d]	ν(C–N)[a] (cm^{-1})	Ref.
$CH_3N{=}S(CH_3)_2$	1208	1.530	812	[16]
$CH_3N{=}SF_2$	1357	1.476	858	[18]
$CH_3N{=}SF_4$	1313	1.495	951 (937)[d]	This work
CH3N=S(F2) =NCH3[b]	$1349_{(o.o.ph)}-1288_{(i.ph)}$[b]	1.483[c]	$890_{(o.o.ph)}-938_{(i.ph)}$[b]	[17]
$CF_3N{=}SF_2$	1384[d]	1.489	816 (807) [d]	[2]
$CF_3N{=}SF_4$	1325[d]	1.503	(858) [d]	This work

[a] gas IR signals.
[b] This molecule presents two $CH_3N{=}S$-moieties, whose stretching modes are strongly coupled. (o.o.ph), out-of-phase stretching; (i.ph), in-phase stretching.
[c] Mean value.
[d] Calculated value, (B3LYP/6-311+G(2df,p)).

values demonstrate a close relationship between these two observables. The longest N=S bond (1.530 Å) and lowest vibrational frequency (1208 cm^{-1}) occur in $CH_3N{=}S(CF_3)_2$. Substitution of the CF_3 groups at sulfur by fluorine atoms causes strong shortening of the S=N bond (1.476 Å) and a corresponding large increase of the frequency (1357 cm^{-1}) in $CH_3N{=}SF_2$. Increase of the oxidation number from S(IV) to S(VI) leads to lengthening of the S=N bond in $CH_3N{=}SF_4$ (1.495 Å) and to lowering of the frequency (1313 cm^{-1}). An intermediate bond length of 1.483 Å (mean value) occurs in the tetracoordinated S(VI) compound $CH_3N{=}S(F_2)$ $=NCH_3$. CH_3/CF_3 substitution at the nitrogen atom in $CH_3N{=}SF_2$ and $CH_3N{=}SF_4$ leads to slight lengthening of the S=N bond by about 0.01 Å and – contrary to the expected trend – to higher vibrational frequencies. Such unexpected relation between bond lengths and vibrational frequencies or force constants, respectively, i.e. increasing force constants with increasing bond lengths has been observed for fluorinated amines and has been rationalized by high bond polarities [18]. Coupling between S=N and C–N vibrations can not explain this increase of ν(S=N) upon CH_3/CF_3 substitution, since ν(C–N) decreases upon this substitution (see below).

The C–N stretching mode of $CH_3N{=}SF_4$ was assigned to the strong IR band centered at 951 cm^{-1} (945 cm^{-1} in Raman). The calculated values for this vibration were 958, 937 and 978 cm^{-1} (HF, B3LYP and MP2, respectively). This fundamental is also sensitive towards substitution at the sulfur atom, since it is strongly coupled with the S=N vibration. However, we assigned the experimental and calculated features to pure C–N and S=N vibrations in order to make the spectral interpretation easier and to allow comparison with other compounds containing the S=N bond. As in the case of the S=N vibration a shift to higher wavenumbers occurs also for ν(C–N) upon substitution of the CF_3 groups in $CH_3N{=}S(CF_3)_2$, (ν(C–N) = 812 cm^{-1} [16]) by more electronegative fluorine atoms in $CH_3N{=}SF_2$ (ν(C–N) = 858 cm^{-1} [19]). In addition, change in sulfur oxidation number from S(IV) to S(VI) also affects the position of this vibration. ν(C–N) increases from 858 cm^{-1} in $CH_3N{=}SF_2$ to 951 cm^{-1} in $CH_3N{=}SF_4$ and from 807 cm^{-1} in $CF_3N{=}SF_2$ to 858 cm^{-1} in $CF_3N{=}SF_4$. For the latter two compounds we use calculated (B3LYP/6-311+G(2df,p)) values, since no experimental value is known for $CF_3N{=}SF_4$. CH_3/CF_3 substitution at nitrogen lowers the C–N vibration from 858 to 816 cm^{-1} (experimental values) in the $=SF_2$ derivatives and from 937 to 858 cm^{-1} (calculated values) in the SF_4 compounds.

The S–F stretching modes belonging to the SF_4 group could be rationalized in terms of four complex vibrations: an asymmetric stretching involving both axial fluorines (F–S–F ax. asym. stretch.), which belongs to the A′ representation, an asymmetric stretching between the two equatorial S–F bonds (F–S–F eq. asym. stretch., (A″)), the symmetric mode involving all four S–F bonds (SF_4 sym. stretch.), which can be defined as the "breathing mode" of the group, and the asymmetric SF_4 stretching mode interpreted as an out-of-phase stretching of the S–F equatorial bonds with respect to the S–F axial bonds. Due to the scarce experimental vibrational data of molecules possessing the SF_4 group, the assignment of these fundamental modes was based only on theoretical predictions. Thus, the asymmetric F–S–F equatorial stretching mode (ν_{13}) was assigned to the strong IR band at 854 cm^{-1} (843 cm^{-1}, very weak in Raman), while the asymmetric F–S–F axial stretching (ν_{16}) was associated with the strongest IR band centered at 816 cm^{-1} (781 cm^{-1}, Raman), in fairly good agreement with the estimated band intensities by all methods (see Table 2). Similarly, the symmetric SF_4 stretching fundamental (ν_{13}) was assigned to the strong IR signal localized at 716 cm^{-1}, whose Raman counterpart was the strongest signal at 710 cm^{-1} and the asymmetric SF_4 stretching mode (ν_{16}) corresponded to the bands observed at 513 and 511 cm^{-1} in the IR and Raman spectra, respectively. The calculated B3LYP/6-311+G(2df,p) wavenumbers for all four stretching vibrations (802, 785, 677 and 522 cm^{-1}) are in close agreement with the experimental values and with those calculated at the same approximation for the related molecules $CF_3N{=}SF_4$, (852, 821, 729 and 555 cm^{-1}) and $FN{=}SF_4$, (814, 839, 720 and 541 cm^{-1}).

In order to simplify the interpretation of the SF_4 deformation modes, they were labelled as NSF eq. out-of-plane deformation; SF_4 symmetric deformation, which is similar to the umbrella movement, NSF_4 wagging, SF eq. rocking, SF ax. rocking and FSF scissoring. This last one involves both equatorial and axial S–F bond deformations coupled out-of-phase. All of them were assigned according to the theoretical predictions. Similarly, the two deformations including the N, S and C atoms, defined as in-plane and out-of-plane bending modes were assigned to the Raman signals observed at 268 and 243 cm^{-1}, respectively.

5. Conclusion

The present analysis allows us to conclude that for molecules possessing the $CH_3N{=}S$ entity two fundamental factors influence the vibrational characteristics of the N=S stretching mode: the electronegativity of the substituents on S and the coordination number of the sulfur atom. Both factors affect the N=S bond length and an inverse relationship between its stretching frequency and the bond length is observed. On the contrary, substitution by a more electronegative group on nitrogen lengthens the N=S bond while increasing the vibrational frequency. Similarly, the C–N stretching mode is also influenced by substitution on sulfur and for compounds possessing the CH_3–N moiety the frequency of the C–N stretching increases in the sequence $CH_3N{=}S(CF_3)_2 < CH_3N{=}SF_2 < CH_3N{=}SF_4$. This vibrational study not only complements the structural analysis for $CH_3N{=}SF_4$, but also starts a new project concerning sulfur–nitrogen systems whose molecular structures, conformational properties and vibrational behaviour can be correlated with our previous results for molecules containing sulfur in oxidation state with IV or VI.

Acknowledgments

Financial support by the Volkswagen Stiftung (I/78 724), DAAD and the Deutsche Forschungsgemeinschaft is gratefully acknowledged. A.G.I., R.M.S.A. and E.H.C. thanks UNT and CONICET, R. Argentina for financial support.

References

[1] R.S.M. Álvarez, E.H. Cutin, R.M. Romano, C.O. Della Védova, Spectrochim. Acta A 52 (1996) 667.

[2] N.L. Robles, E.H. Cutin, C.O. Della Vedova, J. Mol. Struct. 784 (2006) 265.
[3] M.I. Mora Valdez, E.H. Cutin, C.O. Della Védova, R. Mews, J. Oberhammer, J. Mol. Struct. 607 (2002) 207.
[4] R.S.M. Álvarez, E.H. Cutin, C.O. Della Védova, Spectrochim. Acta A58 (2002) 149.
[5] R.S.M. Álvarez, E.H. Cutin, R.M. Romano, C.O. Della Védova, J. Mol. Struct. 443 (1998) 155.
[6] R.S.M. Álvarez, E.H. Cutin, C.O. Della Védova, R. Mews, R. Haist, H. Oberhammer, Inorg. Chem. 40 (2001) 5188.
[7] R. Boese, E.H. Cutin, R. Mews, N.L. Robles, C.O. Della Védova, Inorg. Chem. 44 (2005) 9660.
[8] E.H. Cutin, C.O. Della Védova, H.-G. Mack, H. Oberhammer, J. Mol. Struct. 354 (1995) 165.
[9] R.S.M. Álvarez, M.I. Mora Valdez, C.O. Della Védova, E.H. Cutin, J. Mol. Struct. 657 (2003) 291.
[10] R.M.S. Álvarez, E.H. Cutin, R. Mews, J. Oberhammer, J. Phys. Chem. A 111 (2007) 2243.
[11] H. Günther, H. Oberhammer, R. Mews, I. Stahl, Inorg. Chem. 21 (1982) 1872.
[12] G. Gundersen, K.H. Hedberg, J. Chem. Phys. 51 (1969) 2500.
[13] (a) H. Bock, J.E. Boggs, G. Kleemann, D. Lentz, H. Oberhammer, E.M. Peters, K. Seppelt, A. Simon, B. Solouki, Angew. Chem. 91 (1979) 1008;
(b) H. Oberhammer, J.E. Boggs, J. Mol. Struct. 56 (1979) 107.
[14] R. Mews, Angew. Chem. 90 (1978) 561.
[15] M.J. Frisch, G.W. Trucks, H.B. Schlegel, G.E. Scuseria, M.A. Robb, J.R. Cheeseman, J.A. Montgomery, Jr., T. Vreven, K.N. Kudin, J.C. Burant, J.M. Millam, S.S. Iyengar, J. Tomasi, V. Barone, B. Mennucci, M. Cossi, G. Scalmani, N. Rega, G.A. Petersson, H. Nakatsuji, M. Hada, M. Ehara, K. Toyota, R. Fukuda, J. Hasegawa, M. Ishida, T. Nakajima, Y. Honda, O. Kitao, H. Nakai, M. Klene, X. Li, J.E. Knox, H.P. Hratchian, J.B. Cross, C. Adamo, J.Jaramillo, R. Gomperts, R.E. Stratmann, O. Yazyev, A.J. Austin, R. Cammi, C. Pomelli, J.W. Ochterski, P.Y. Ayala, K. Morokuma, G.A. Voth, P. Salvador, J.J. Dannenberg, V.G. Zakrzewski, S. Dapprich, A.D. Daniels, M.C. Strain, O. Farkas, D.K. Malick, A.D. Rabuck, K. Raghavachari, J.B. Foresman, J.V. Ortiz, Q. Cui, A.G. Baboul, S. Clifford, J. Cioslowski, B.B. Stefanov, G. Liu, A. Liashenko, P. Piskorz, I. Komaromi, R.L. Martin, D.J. Fox, T. Keith, M.A. Al-Laham, C.Y. Peng, A. Nanayakkara, M. Challacombe, P.M.W. Gill, B. Johnson, W. Chen, M.W. Wong, C. Gonzalez, J.A. Pople, Gaussian 03, Revision B.03, Gaussian, Inc., Pittsburgh PA, 2003.
[16] F. Trautner, R.M.S. Alvarez, E.H. Cutin, N.L. Robles, R. Mews, H. Oberhammer, Inorg. Chem. 44 (2005) 7590.
[17] N.L. Robles, E.H. Cutin, R. Mews, H. Oberhammer. submitted for publication.
[18] H.-G. Mack, D. Christen, H. Oberhammer, J. Mol. Struct. 190 (1988) 215.
[19] B. Cohen, A.G. MacDiarmid, J. Chem. Soc. (A) (1966) 1780.